Published in final edited form as:
Cell. 2012 May 11; 149(4): 832–846. doi:10.1016/j.cell.2012.03.032.

Nuclear envelope budding enables large ribonucleoprotein particle export during synaptic Wnt signaling

Sean D. Speese[*,+], **James Ashley**[*,+], **Vahbiz Jokhi**[*], **John Nunnari**[*], **Romina Barria**[*], **Yihang Li**[*], **Bulent Ataman**[*], **Alex Koon**[*], **Young-Tae Chang**[@], **Qian Li**[&], **Melissa J Moore**[†], and **Vivian Budnik**[*]

[*]Department of Neurobiology, University of Massachusetts Medical School, Worcester, MA 01605

[†]RNA and Neuro Therapeutics Institutes, Department of Biochemistry and Molecular Pharmacology, Howard Hughes Medical Institute, University of Massachusetts Medical School, Worcester, MA 01605

[&]Department of Chemistry, New York University, New York, New York 10003

[@]Department of Chemistry & Med Chem Program, National University of Singapore, and Laboratory of Bioimaging Probe Development, Singapore Bioimaging Consortium, A*STAR, Biopolis, Singapore

SUMMARY

We report a novel mechanism of ribonucleoprotein (RNP) nucleocytoplasmic export by nuclear envelope budding. During development of *Drosophila* synapses, a fragment of the Wnt-1 receptor, DFrizzled2, is imported into postsynaptic nuclei where it forms prominent foci. We now show these foci to be composed of large RNP granules harboring synaptic protein transcripts. These RNPs exit the nucleus via a budding mechanism akin to nuclear egress of Herpes-type viruses, a process previously thought to be exclusive to these viruses. During this mechanism, RNP granules bud into the space between the inner and the outer nuclear membranes (the perinuclear space), in a manner dependent on Lamin C, a nuclear protein linked to muscular dystrophies. Like herpes

Correspondence to: Melissa J Moore; Vivian Budnik.

[+]These authors contributed equally to the work

Authors' contributions to the paper:

Dr. Sean D. Speese carried out and designed many of the experiments, and was a critical intellectual contributor to the project and writing the paper.
Dr. James Ashley was responsible for the FISH data and live imaging, contributed intellectually and helped edit the manuscript.
Mr. John Nunnari carried out all the EM experiments.
Ms. Romina Barria supported the work of Drs. Speese and Ashley by helping with immunocytochemical procedures, NMJ morphometry, FISH, and Western blots.
Ms. Vahbiz Jokhi Carried out the experiments with aPKC, and contributed intellectually to experimental design.
Ms. Yihang Li carried out the Lamin Immunopurifications.
Dr. Bulent Ataman was the first to discover that nuclear DFz2C foci where localized at LamC foci, and that synaptic activity regulated the number of LamC foci in conjunction with DFz2C foci.
Mr. Alex Koon carried out the live imaging of RNA particles labeled with E36.
Dr. Young-Tae Chang supplied the E36 dye for live imaging.
Dr. Qian Li synthesized the E36 dye,
Dr. Melissa J Moore provided instrumental intellectual input, contributed to experimental design, and collaborated in writing the manuscript.
Dr. Vivian Budnik directed the project and contributed to experimental design, discussions and manuscript writing.

virus nuclear egress, this process requires protein kinase C, which is known to disrupt the lamin through phosphorylation. We suggest that nuclear budding is an endogenous nuclear export pathway for large RNP granules.

INTRODUCTION

Wnts are secreted signaling proteins important for embryonic pattern formation and cellular differentiation(Siegfried and Perrimon, 1994), and also play pivotal roles during activity-dependent synaptic development (Budnik and Salinas, 2011; Speese and Budnik, 2007). In mammals, Wnts promote synapse differentiation and plasticity and contribute to neuronal excitability (Budnik and Salinas, 2011; Cerpa et al., 2011; Varela-Nallar et al., 2010). At the *Drosophila* larval neuromuscular junction (NMJ) the Wnt-1, Wingless (Wg), is released by presynaptic boutons in a manner regulated by neuronal activity, and is critical for proper synaptic bouton differentiation (Ataman et al., 2008; Packard et al., 2002). In the absence of Wg signaling, NMJs fail to expand properly during larval development (Miech et al., 2008; Packard et al., 2002). Further, a subset of synaptic boutons (ghost boutons) is devoid of active zones and postsynaptic structures, and fail to recruit postsynaptic proteins (Ataman et al., 2006; Packard et al., 2002). Wg release by motorneurons activates alternate transduction pathways in motorneurons and muscles (Mathew et al., 2005; Miech et al., 2008). In postsynaptic muscles, Wg turns on the Frizzled Nuclear Import (FNI) pathway in which the Wg receptor, DFrizzled-2 (DFz2), is internalized and transported to muscle nuclei (Ataman et al., 2006; Mathew et al., 2005). Subsequently, a C-terminal cleavage product, DFz2C, is imported into the nucleus (Mathew et al., 2005) via canonical nuclear import machinery (Mosca and Schwarz, 2010) where it localizes to discrete foci (Ataman et al., 2008; Mathew et al., 2005). A similar transduction pathway has been reported for the Wnt receptor Ryk during mammalian cortical neuron development (Lyu et al., 2008). However, the nuclear function of these DFz2C/Ryk C-terminal fragments remains unexplored.

We report that FNI signaling leads to nuclear DFz2C fragments being organized into ribonucleoprotein particles containing mRNAs encoding postsynaptic proteins. These particles exit the nucleus via a mechanism akin to the nuclear egress of herpes virus capsids. In viral capsid egress, the nuclear lamina is disrupted through phosphorylation by protein kinase C (PKC), which is required for the budding of an inner nuclear membrane (INM) bound viral particle into the perinuclear space (between the INM and the outer nuclear membrane; ONM). Subsequent fusion of the INM surrounding the virus with the ONM releases the naked viral capsid into the cytoplasm. We find that localization of DFz2C granules to the perinuclear space requires the A-type Lamin, LamC. Further, formation of INM invaginations, through which the DFz2C granules exit, requires atypical PKC (aPKC), which likely phosphorylates LamC. Significantly, disruption of this process leads to phenotypes paralleling those observed in laminopathy models. Our studies thus provide evidence for a novel mechanism by which cellular mRNAs can exit the nucleus, insight into the mechanisms of postsynaptic apparatus assembly in response to Wnt signaling, and a potential explanation for how certain human lamin mutations result in muscular dystrophy.

RESULTS

DFz2C and Lamin C form specializations at the nuclear lamin

To elucidate the nuclear function of DFz2C, we sought to determine the subnuclear localization of DFz2C foci in muscle cells (Fig.1; SF1). DFz2C foci localized to the nuclear periphery (Fig.1A) and consisted of accumulations of discrete DFz2C puncta (Fig.1A; arrows; SF1A; see also SF1C for a salivary gland DFz2C nuclear focus). Co-labeling with antibodies to the *Drosophila* A-type lamin, LamC, a component of the nuclear lamina that

forms a lattice beneath the INM, revealed that LamC forms “framework-like” structures surrounding the DFz2C puncta (Fig.1A; SF1B). These structures were even more apparent upon structured illumination (SF1B). Thus, DFz2C fragments are associated with a specialization of the nuclear lamina.

Formation of DFz2C foci was dependent on LamC, as null mutants in *lamC* virtually eliminated DFz2C foci (Fig.1B). Likewise, LamC foci depended on DFz2, as mutations in *dfz2*, downregulation of *dfz2*, or DFz2 overexpression [which behaves as a dominant negative (Mathew et al., 2005; Packard et al., 2002) significantly decreased the number of LamC foci (Fig.1B). Further, both DFz2C and LamC foci were significantly upregulated in the hyperexcitable K^+ channel double mutant *eag Sh*, which exhibits increased synaptic activity (Wu et al., 1983) (Fig.1B). This parallels previous data showing that the number of nuclear DFz2C foci correlates with synaptic activity (Ataman et al., 2008). Thus, DFz2C foci and LamC framework-like structures are mutually dependent for their formation, and synaptic activity leads to analogous changes in their numbers.

Mutations in the human *LMNA* gene lead to a diverse set of disorders, including muscular dystrophies such as autosomal dominant Emery-Dreifuss muscular dystrophy (AD-EDMD) (Burke and Stewart, 2002; Mejat et al., 2009; Ostlund et al., 2001). Expression of the AD-EDMD mutant protein results in formation of LMNA-positive "O-ring" structures in the nucleus and the same structures are also observed when expressing a mutant *lamC* transgene modeled after the human mutant gene (Ostlund et al., 2001; Schulze et al., 2005). Notably, we also observed nuclear O-ring structures in the muscles of *Drosophila* larva heterozygous for a LamC-GFP-trap ($lamC^{GFP\text{-}trap/+}$), in which GFP is inserted in frame within the region encoding the LamC rod domain (Morin et al., 2001) (Fig.1C). In this strain, we found that both DFz2C and LamC-GFP acquired the form of an O-ring, and both the appearance of DFz2C as individual granules and LamC as a framework surrounding the granules was lost (Fig.1C). This suggests that insertion of GFP within the rod domain in $lamC^{GFP\text{-}trap}$ alters the normal behavior of the protein, and underscores the dependence of DFz2C foci on wild type LamC.

The strong dependence of DFz2C foci on normal LamC predicts that mutations in *lamC* should elicit phenotypes resembling those of mutations disrupting the FNI Wnt signaling pathway. Consistent with this, *lamC* null mutants, larvae expressing LamC-RNAi in muscle and $lamC^{GFP\text{-}trap/+}$ larvae all exhibited a significant increase in the number of “ghost boutons” (Fig.1D–J), undifferentiated synaptic boutons that are a hallmark of FNI pathway disruption, including mutations that block importin-mediated nuclear import of DFz2C (Ataman et al., 2006; Mosca and Schwarz, 2010; Packard et al., 2002). Ghost boutons lack the entire complement of postsynaptic proteins, including the PSD-95 homolog, Discs-Large (DLG) (Fig.1F–I), and glutamate receptors. In both *lamC* null animals and those expressing LamC-RNAi in muscles, synaptic arbors were morphologically disrupted, being composed of enlarged tubular boutons instead of the normal small “beads on a string”(Fig.1L; SF1K). This phenotype is also observed in *wg* mutants (Packard et al., 2002). Like other mutations affecting the FNI pathway, *lamC* null mutants also exhibited a decrease in the number of mature boutons (Fig.1K; SF1L). Recent evidence in mice indicates that NMJ defects precede muscle degeneration during laminopathies (Mejat et al., 2009). Consistent with this, in *lamC* mutants we detected only defects at the NMJ and no gross defects in larval body wall muscle architecture at muscles 6 and 7 (abdominal segments A2 and A3), where the NMJ analysis was conducted (SF1D–I).

Synaptic transmission was also altered in a similar manner in *lamC* and *dfz2* mutants, as well as upon overexpressing DFz2 in muscles, conditions that severely reduce the number of DFz2C/LamC foci. In the above genotypes, the frequency of spontaneous miniature

excitatory junctional potentials (mEJPs) was significantly increased (Fig. 1M; SF1M). The amplitude of mEJPs was also increased in these strains (Fig. 1N; SF1M), suggesting a defect in postsynaptic receptors. This suggestion was supported by morphological analysis of GluRIIA clusters, which showed an increase in volume and total signal intensity (Fig.1P–S). Nevertheless, the amplitude of EJPs was normal (Fig.1O; SF1N). This is not surprising, as larval NMJs are capable of homeostatic compensation as a result of changes in postsynaptic activity (Petersen et al., 1997). A slightly different profile was observed in $lamC^{GFP\text{-}trap/+}$ larvae, in which DFz2C/LamC foci are still present, albeit with abnormal morphology. Although mEJP amplitude was increased (Fig.1N; SF1M), mEJP frequency was unaltered (Fig.1M; SF1M) and EJP amplitude showed a small but significant decrease compared to wild type controls (Fig.1O; SF1N). Taken together, our results indicate that the nuclear lamina plays a specific role in synapse development and function by participating in the FNI signaling pathway in postsynaptic muscles.

DFz2C granules are localized at invaginations of the inner nuclear membrane

The association of DFz2C foci with the nuclear periphery and their dependence on LamC is suggestive of a specialized function of the nuclear lamina. Vertebrate A-type lamins are known to form foci at sites of DNA replication (Kennedy et al., 2000). However, DNA was undetectable at the DFz2C/LamC foci as determined by co-labeling with DNA markers (Fig. 2A,B; SF1J; N=30 foci). LamA/C also localizes to and is required for expansion of the nucleoplasmic reticulum (NR), double-walled invaginations of the nuclear envelope involved in signaling and transport (Gehrig et al., 2008; Lagace and Ridgway, 2005). NR contain both the inner (INM) and outer (ONM) nuclear membranes and are labeled by markers of the nuclear pore complex (Lagace and Ridgway, 2005). Using membrane markers, we found that 92% of the DFz2C foci were wrapped by nuclear membrane (Fig. 2C; SF2A,B; N= 60 DFz2C foci), but unlike the NR, DFz2C foci were not coincident with nuclear pore complexes (Fig.2E; N= 35 DFz2C foci).

The NR define lumens projecting into the nucleus but continuous with the cytoplasm, as revealed by cytoplasmic injection of fluorescent dextrans with molecular masses above the cutoff for passive diffusion through nuclear pores (~40 kDa) (Keminer and Peters, 1999; Lagace and Ridgway, 2005). However, we observed no association between DFz2C/LamC foci and a Texas Red-conjugated 70 kDa dextran injected into muscle cells (Fig.2D; N= 40 DFz2C foci). Thus DFz2C/LamC foci are not within reticuli continuous with the cytoplasm. Instead they are located within the perinuclear space (between the INM and ONM).

Yet another type of nuclear membrane invagination is INM infolding. Such INM infoldings occur during nuclear egress of herpes viruses (e.g. HSV and CMV) in mammalian cells (Buser et al., 2007; Darlington and Moss, 1968). Herpes viral particles are assembled in the nucleus and are far too large to be exported through nuclear pores. Instead, they become enveloped by the INM as they bud into the perinuclear space (SF3H). This is followed by a de-envelopment process, in which the INM-derived envelope fuses with the ONM, releasing the naked nucleocapsids into the cytoplasm (Lee and Chen, 2010).

To determine if DFz2C/LamC foci correspond to INM infoldings, we carried out an ultrastructural analysis (Fig.3). In electron micrographs (EMs) we could routinely observe nuclear membrane invaginations bounded by a single membrane, likely the INM (Fig.3A, B; N= 7 preparations; 9 foci). We also observed large electron-dense granules (average diameter = 192±0.01 nm: min/max 143/286; N=31 granules from 7 foci) (Fig.3A, B), located within the enlarged perinuclear space bounded by these INM invaginations (Fig.3A, B). Similar INM invaginations were also observed in a Schneider-2 (S2) cell line endogenously expressing DFz2 and Wg, which also display nuclear DFz2C foci (Fig.3C,D). Similar to muscle, S2 cells can also import DFz2C into the nucleus in the presence of Wg

(Mathew et al., 2005). DFz2C antibody labeling of these electron dense granules in larval muscle cells, confirmed that they correspond to the DFz2C foci observed at the light microscopy level (Fig.3F,H; SF3A,C; N=29 animals; 93 foci).

The DFz2C granules within the INM invaginations appeared to be bounded by membrane (Fig.3D; arrow). If these granules are enveloped by the INM, then Lamin immunoreactivity could surround the dense granules. Indeed, LamC immunoreactivity lined the outer edge of the DFz2C granules (Fig.3E,G; SF3B; N= 29 animals; 93 foci), which correlates well with our observations of DFz2C/LamC foci at the light level.

Some DFz2C foci were also associated with ONM evaginations highly reminiscent of herpes nucleocapsids emerging from the nuclear envelope (Buser et al., 2007) (SF3D–F,H; arrows). Such evaginations often contained DFz2C electron dense granules (SF3D; asterisks), but some were devoid of granules (SF3E,F), as has been observed after HSV egress from the perinuclear space (Buser et al., 2007; Granzow et al., 2001). Consistent with this idea, we also observed electron dense granules in the cytoplasm, close to the evaginations (SF3E; arrowhead). At the light level, evaginations of the lamina containing DFz2C labeling were also observed (SF3I). Thus, DFz2C foci are composed of electron dense, DFz2C- and LamC-associated granules that localize within the perinuclear space and are bounded by the INM. Further, these granules appear to be released into the cytoplasm either by evagination of the ONM or fusion of an INM bound granule localized to the perinuclear space, with the ONM (SF3H). Interestingly, in *lamC*$^{GFP\text{-}trap/+}$, in which DFz2C/LamC foci are morphologically disrupted, foci appeared as large electron dense and amorphous structures associated with the nuclear envelope, in which no individual DFz2C granules could be distinguished (SF3G; arrows).

DFz2C/LamC foci contain RNAs that exit the nucleus

Whereas HSV nucleocapsids contain dsDNA, DFz2C/LamC foci occur in DNA-free regions (Fig.2AB). To determine if the DFz2C-immunoreactive granules contained RNA, we screened the *Drosophila* flytrap database for fly stains expressing GFP fused in-frame with endogenous proteins involved in RNA binding, maturation or localization (34 strains; Suppl. Table 1), and determined if any such GFP fusion proteins localized at or near DFz2C/LamC foci. One such strain contained GFP fused in-frame with endogenous Poly(A) Binding Protein 2 (PABP2/PABPN1). In PABP2-GFP muscle nuclei GFP signal was observed both as diffuse nucleoplasmic fluorescence expected for PABP2 and bright GFP foci at the nuclear periphery (Fig.4A). This was distinct from the localization of NLS-GFP when expressed with a muscle Gal4 driver, which yielded diffuse staining throughout the nucleoplasm (SF4B,C; of 498 LamC foci examined in 6 animals, 0% showed discrete NLS-GFP enrichment at the foci). The GFP distribution in PABP2-GFP larval nuclei was similar to the endogenous PABP2 distribution revealed by labeling wild-type larvae with an antibody against *Drosophila* PABP2 (Benoit et al., 1999) (SF4A). About 40% of the bright PABP2-GFP foci were juxtaposed with DFz2C/LamC foci and 32% of the DFz2C foci were juxtaposed with a bright PABP2 focus (N=118 foci). Further, there was a significant positive correlation between the number of PABP2 and DFz2C foci per nucleus (SF4D; R= 0.52; $p<0.0001$). Further, the presence of bright PABP2 foci was dependent both on LamC and DFz2C, as both the *lamC* null mutation and a strong *dfz2* loss of function mutation drastically decreased the number of PABP2 foci (Fig.4B). This suggests that the PABP2 foci are formed in conjunction with DFz2C/LamC foci.

PABP2 binds to the short poly(A) tail of immature transcripts in the nucleus, promoting poly(A) tail elongation by poly(A) polymerase (Kuhn et al., 2009). To determine if DFz2C granules contained polyadenylated RNA we conducted fluorescent in-situ hybridization (FISH) with Digoxigenin-conjugated oligo-dT. 64% of the LamC foci contained high oligo-

dT fluorescence (Fig.4C; N=25 foci in 6 preparations) and the signal was completely eliminated by RNAse treatment (Fig.4D; 0% of LamC foci contained oligo-dT fluorescence; N=26 foci in 6 preparations).

The presence of RNA at the foci was additionally supported by performing Bernhard's regressive EDTA (rEDTA) stain on thin sections. This procedure chelates the electron dense uranyl acetate label from DNA, but not from RNA (Bernhard, 1969), as evidenced by the preferential retention of electron dense staining in the ribosomes dotting the nuclear envelope (Fig.4E1, arrowhead) and in the cytoplasm (Fig.4E1,E3,F1,F3), and its near elimination from DNA (Fig.4E2,F2). Notably, the large electron dense granules at the nuclear periphery were resistant to EDTA treatment (Fig.4E1,F1,G). Taken together, these data indicate that DFz2C granules contain RNA, and at least some of these RNAs are polyadenylated.

In rEDTA EM mages, we also observed electron dense granules similar to DFz2C granules in the cytoplasm close to the nuclear envelope (Fig.4G; arrows), supporting the idea that DFz2C granules are released from the perinuclear space into the cytoplasm. To directly monitor whether RNA granules found at the DFz2C/LamC foci were released into the cytoplasm, we conducted live imaging of foci from larval body wall muscle preparations, using the RNA-specific dye E36 (Li et al., 2006). Fluorescent granules emerging from nuclei in E36-labeled preparations were imaged blind and then fixed and labeled with antibodies to LamC and DFz2C. Images from the fixed preparations were then sized and superimposed to the live images using fiduciary markers (Fig.5A,B; Suppl. Movie 1, 2). E36-positive aggregates and granules were observed in both nucleus and cytoplasm. Close examination revealed E36-positive puncta emerging from the LamC foci and exiting the nucleus. Thus, at least some of the foci-associated RNA granules translocate to the cytoplasm.

Atypical Protein Kinase C is required for DFz2C/LamC foci formation

HSV nucleocapsids recruit a host protein kinase C (PKC), which phosphorylates A and B-type Lamin, disrupting the nuclear lamina at the INM and allowing the capsid to bud into the perinuclear space (Park and Baines, 2006). The PKC involved in this process is likely not a conventional PKC (Leach and Roller, 2010). Notably, we observed that a binding partner of *Drosophila* atypical PKC (aPKC), Bazooka (Baz)/Par3, colocalized with LamC, both in the nuclear lamina and at foci (Fig.6A). Low levels of aPKC immunoreactivity were also detected inside the nucleus (Fig.6B). These observations raised the possibility that aPKC might be involved in remodeling the lamina around INM invaginations defining DFz2C/LamC foci. To test this, we modified aPKC activity in muscles. Expressing aPKC-RNAi in muscles nearly eliminated DFz2C/LamC foci (Fig.6C,D,J), suggesting that aPKC is required for foci formation. This conclusion was supported by pharmacological experiments showing that feeding larvae with chelerythrine, a PKC inhibitor (Herbert et al., 1990), significantly reduced DFz2C/LamC foci number (Fig.6E,J). Conversely, increasing aPKC activity by expressing PKM in muscles dramatically increased both the size and number of LamC foci (Fig.6F,J), suggesting that increasing aPKC activity promotes LamC foci formation. However, these foci were completely devoid of DFz2C signal (Fig.6F). Thus, although constitutively activating aPKC throughout larval development promotes reorganization of the lamina, it prevents normal loading of LamC foci with DFz2C granules. To both limit PKM expression and allow for temporal control of its delivery, we expressed PKM under control of the heat-shock promoter (hs-PKM). At permissive temperature hs-PKM larvae displayed an increase in the number of DFz2C/LamC foci compared to wild type, likely due to the known leakiness of the hs promoter (Fig.6J; (Hans et al., 2011)). A much larger increase in DFz2C/LamC foci was produced by a 30 min heat shock at 30°C followed by 2 hr at permissive temperature prior to dissection (Fig.6G,J), while no significant change in

DFz2C/LamC foci number was elicited in wild type controls subjected to the same protocol (Fig.6J). In these larvae, LamC foci also contained DFz2C immunoreactivity (Fig.6G), consistent with the idea that while chronic PKM expression interferes with DFz2C foci formation, acute PKM activation allows for normal formation of DFz2C granules within LamC foci.

Labeling body wall muscles with an antibody specific for phosphorylated PKC substrates (P-PKCs (Zhang et al., 2002)) resulted in intense immunoreactivity at the foci (Fig.6H), and treatment of the samples with lambda-phosphatase eliminated this signal (Fig.6I). No such accumulations of P-PKCs signal were observed in larvae expressing aPKC-RNAi in muscles (SF5A). Western blotting of body wall muscle extracts with the P-PKCs antibody revealed a band at the same molecular weight as LamC (Fig.6L). The intensity of this band increased in larvae expressing PKM in muscles and, conversely, it decreased when aPKC-RNAi was expressed in muscles (Fig.6L). Consistent with the idea that this band corresponded to LamC, immunoprecipitation of body wall muscle extract with LamC antibodies revealed that LamC is recognized by P-PKCs antibody (Fig.6M). Further, the intensity of this band, when the blots were probed with anti-P-PKCs, was increased in LamC immunoprecipitates from larvae expressing PKM in muscles (Fig.6M). Taken together, the above results suggest that PKC-dependent phosphorylation is necessary and sufficient to locally remodel the lamina in order to form DFz2C/LamC foci. Downregulating the aPKC-binding partner, Baz/Par3, by expressing Baz-RNAi in muscles, virtually eliminated the foci (Fig.6J), suggesting that Baz might function in conjunction with aPKC.

We next assessed whether altering aPKC activity or Baz levels elicits ghost bouton formation. Previous studies demonstrated that both downregulation and constitutive activation of aPKC, as well as downregulation of Baz, leads to a reduction in the number of synaptic boutons at the NMJ, partly due to a local function of these proteins in cytoskeletal regulation at the NMJ (Ramachandran et al., 2009; Ruiz-Canada et al., 2004). However, whether ghost boutons were formed in the above genotypes was not tested. We downregulated aPKC or Baz or expressed PKM, all specifically in muscles. NMJs in all of the above genotypes displayed a significant increase in the number of ghost boutons (Fig. 6K). Thus, like mutations that interfere with DFz2C foci formation, manipulations in aPKC and Baz lead to the formation of undifferentiated boutons.

DFz2C/LamC foci contain synaptic protein transcripts

We next sought to identify specific mRNAs trafficked through the foci, possibly for local translation at postsynaptic sites. Using a candidate approach for mRNAs encoding known postsynaptic proteins and others involved in nervous system development, we identified 6 transcripts localizing to the foci among 19 mRNAs tested (Suppl. Table 2). Of these, the PDZ protein Par6 was selected for further study (Fig.7). Par6 is part of a tripartite protein complex, consisting of Baz, Par6, and aPKC (Betschinger et al., 2003). At the *Drosophila* NMJ all three proteins localize both pre- and postsynaptically (Ruiz-Canada et al., 2004), and both Baz and aPKC have been implicated in cytoskeleton remodeling during synaptic growth (Ramachandran et al., 2009; Ruiz-Canada et al., 2004). In addition to colocalizing with nuclear LamC foci (Fig.7A), Par6 mRNA was observed in puncta near folds of the lamina, where LamC foci were not yet apparent (Fig.7B). These could represent granules in the process of formation prior to their translocation into the perinuclear space. Notably, we also observed Par6 mRNA granules within evaginations of the nuclear lamina (Fig.7C,D), likely representing the nuclear envelope evaginations observed at the ultrastructural and light microscopy levels (SF3D–F,I). The nuclear Par6 *in situ* signal was specific, as no signal was observed with a non-muscle probe, wg (Fig.7G;SF5E), and expressing Par6-RNAi in muscle virtually eliminated the nuclear *par6* hybridization signal (SF5B,C).

In S2 cell extracts, an antibody against the C-terminus of DFz2 immunoprecipitated Par6 mRNA but not an mRNA (Mad) absent from DFz2C foci (Fig.7M; Suppl. Table 1). The Par6 primers used were in adjacent exons and the RT-PCR product was of the size expected from spliced mRNA. The identity of the RT-PCR product was confirmed by sequencing. Thus the Par6 RNA associated with DFz2C is spliced, suggesting that it is mature.

The presence within DFz2C granules of mRNAs encoding postsynaptic apparatus components raises the possibility that these granules are trafficked to the NMJ where the mRNAs within are locally translated, as has been demonstrated for RNA granules in neurons (Wang et al., 2010). Indeed, local translation of GluRs has been reported at the NMJ (Sigrist et al., 2000) and the SSR contains polyribosomes ((Sigrist et al., 2000); SF6). Using two different Par6 probes we found that Par6 mRNA was associated with the NMJ (Fig.7H–J) and no signal was observed with a *wg* probe (Fig.7K). The NMJ Par6 signal was virtually eliminated upon expressing LamC-RNAi in muscles (Fig.7L) confirming the specificity of the signal. Further, ghost boutons present in *lamC* mutants were devoid of postsynaptic Par6 protein, and showed a marked decrease in overall postsynaptic Par6 levels (Fig.7E,F). Taken together these data suggest that proper localization and local translation of at least one postsynaptic transcript, Par6, requires the FNI pathway.

DISCUSSION

The canonical view of nucleocytoplasmic transport posits that the sole gateway into and out of the nucleus is the nuclear pore complex (NPC). Thus all RNAs and RNPs synthesized and assembled in the nucleus are thought to access the cytoplasm by transiting the NPC. Our study now provides evidence for an alternative RNP export pathway: nuclear envelope budding. We uncovered this pathway while investigating Wnt-dependent NMJ synapse development in *Drosophila* larval body wall muscles. We find that C-terminal fragments of the Wg receptor DFz2 accumulate in nuclear foci in association with large RNA granules localizing to the space between the INM and ONM. These granules are found at sites of INM invaginations, are bounded by LamC, and can be seen leaving the nucleus. Further, the granules contain transcripts encoding postsynaptic proteins, and mutations interfering with foci formation prevent proper differentiation of synaptic boutons. Thus we suspect that, after exiting the nucleus by budding, the DFz2C RNP granules translocate to sites of synapse formation where local translation of the encoded proteins contributes to synapse assembly.

In addition to describing a novel pathway for nuclear export of endogenous RNPs, our work sheds light on the previously mysterious mechanisms by which mutations in nuclear lamins and INM proteins lead to muscular dystrophies and related movement disorders (Burke and Stewart, 2002; Mejat et al., 2009). Further, by showing that nuclear import of a membrane receptor fragment serves to promote export of mRNA transcripts, this work adds a novel twist to the molecular mechanisms governing membrane to nucleus communication in Wnt signaling pathways.

Nuclear envelope budding and herpes viral egress

The nuclear budding pathway described here bears remarkable resemblance to the nuclear egress mechanism employed by herpes viruses. Herpes capsids containing dsDNA are assembled in the nucleus, where they form multimegadalton complexes much too large to pass through NPCs. Instead, they exit via INM envelopment and ONM de-envelopment (Fig.SF3H)(Lee and Chen, 2010; Roller, 2008). Until now this highly unusual nuclear export pathway had been thought unique to this family of viruses, and not representative of any endogenous nuclear export pathway (Roller, 2008). Rather it was supposed that herpes viruses had hijacked the lamina disassembly pathway operational during nuclear replication (Haas and Jost, 1993).

Both herpes virus egress and replication-dependent nuclear envelope disassembly involve multiple phosphorylation events (Roller, 2008). In capsid egress, viral proteins pUL34 and pUL31 are targeted to the INM where they recruit viral pUS3 kinase and host PKCs (Park and Baines, 2006; Reynolds et al., 2004; Ryckman and Roller, 2004). Both pUS3 and the host PKCs disrupt the nuclear lamina by phosphorylating lamins, including LMNA, and other lamina-associated proteins (Bjerke and Roller, 2006; Leach and Roller, 2010; Milbradt et al., 2010). Both pUL34 and pUL31 have also been suggested to induce INM curvature around the capsid, facilitating budding into the perinuclear space (Klupp et al., 2007).

We present multiple lines of evidence supporting the idea that local lamina remodeling at sites of DFz2C granule formation is driven by the same mechanisms at work in viral capsid egress and that these mechanisms have profound implications for synapse development. First, atypical PKC is required for both lamina remodeling and formation of INM invaginations containing DFz2C granules (Fig.6D–F, J). Second, the apparent phosphorylation level of a species with identical electrophoretic mobility to LamC paralleled changes in aPKC activity (Fig.6L), and this same band was immunoprecipitated with antibodies to LamC (Fig.6M). Third, the aPKC recruitment factor Baz also localized to DFz2C/LamC foci (Fig.6A), and Baz downregulation in muscles prevented DFz2C/LamC foci formation (Fig.6J). Fourth, altered aPKC activity through RNAi or expression of a constitutively active enzyme, as well as decreasing Baz levels, resulted in an increase in ghost bouton number (Fig. 6K), similar to other disruptions of the FNI pathway (Fig. 1J). Fifth, downregulation of the FNI pathway through LamC-RNAi, or DFz2 overexpression in muscles, led to an increase in GluRIIA clustering similar to that observed in mutations in *dapkc* and *baz* (Fig. 1P–S and Ramachandran et al 2009; Ruiz-Canada et al 2004). This increase in GluR clustering was reflected by an elevation of mEJP amplitude (Fig. 1N), as also observed in *dapkc* and *baz* mutants. Finally, immunofluorescence from an antibody recognizing phosphorylated PKC substrates was greatly enhanced at DFz2C/LamC foci (Fig.6H, I). Thus we propose that herpes viruses have in fact hijacked a nuclear export pathway employed by endogenous RNPs.

Other reports of perinuclear granules

That nuclear envelope budding has not been previously investigated as a means for endogenous RNP egress raises the question of whether this is a highly specialized mechanism utilized only by *Drosophila* larval muscle cells, or is a more widespread phenomenon. Our results and reports in the literature strongly support the latter view. Notably, we observed DFz2C/LamC foci in both *Drosophila* salivary gland (Fig.SF1C) and in S2 cell nuclei (Fig.3C, D), both of which appear to utilize the FNI signaling pathway. Others have also reported INM infoldings containing electron dense granules (suggested to be aggregates of RNPs) in *Drosophila* salivary glands and midgut cells at specific developmental stages (Gay, 1956; Hochstrasser and Sedat, 1987). Similar perinuclear granules have likewise been observed in diverse contexts, from plants (Dickinson, 1971) to mammals, where they are particularly prevalent in early embryonic stages (Hadek and Swift, 1962; Szollosi, 1965). Indeed, that such granules might reflect an alternate mode of nucleocytoplasmic export has been previously proposed (Gay, 1956; Szollosi and Szollosi, 1988), but it had not been experimentally validated until now. The combination of our data with the numerous cytological reports of perinuclear granules strongly supports the notion that nuclear envelope budding is a mechanism for nuclear export of large RNP granules in many cell types.

Congenital neuromuscular diseases and nuclear budding

Mutations across the human *LMNA* gene lead to a diverse set of disorders (Burke and Stewart, 2002) termed laminopathies, with extreme variability in their tissue specificity and

pathogenesis. Some manifest as muscular dystrophies affecting specific skeletal muscles (Burke and Stewart, 2002; Mejat et al., 2009). While laminopathies affecting muscles have been historically classified as myopathies, recent evidence in mice indicates that gross NMJ defects are detectable well before any signs of muscle degeneration (Mejat et al., 2009). Similarly, we observed no alterations in *Drosophila* larval muscle morphology or organization in the same *lamC* mutants wherein defects at the NMJ were clearly evident (Fig.1F–L, SF1L). Thus, the underlying basis of many muscle-specific laminopathies could be disruption of nuclear budding leading to improper NMJ development. Consistent with this are observations that insertion of GFP sequences in the highly conserved rod domain of fly LamC (this report and (Schulze et al., 2009)) results in formation of LMNA-positive "O-ring" structures in the nucleus, as well as disruption of both DFz2C granule organization and NMJ development. Similar O-rings have been observed in humans with autosomal dominant Emery-Dreifuss muscular dystrophy (AD-EDMD) (Ostlund et al., 2001; Schulze et al., 2009), which is caused by mutations in this same rod domain.

An additional link between congenital neuromuscular disease and nuclear budding is provided by studies of Dystonia, a sustained muscle contraction disorder (Robottom et al., 2011). Dystonia symptoms are ameliorated by botulinum toxin treatment (Lim and Seet, 2010), suggesting defects in neurotransmission. The AAA+ ATPase TorsinA is responsible for most cases of early-onset autosomal-dominant primary dystonia (Breakefield et al., 2001). Besides its role in synaptic vesicle recycling (Granata et al., 2008), a recent study indicates that TorsinA is required for HSV nuclear egress (Maric et al., 2011). Moreover, ultrastructure analysis of developing motorneurons in *torsinA* mutant mice revealed accumulations of vesicular structures in the perinuclear space (Goodchild et al., 2005). Taken together, these results raise the intriguing possibility that TorsinA functions to promote nuclear envelope scission during nuclear budding, and that alterations in RNP granule export might contribute to the phenotypic characteristics of Dystonia.

Role of DFz2C granules in synapse development

We identified several transcripts colocalizing with DFz2C/LamC foci encoding postsynaptically localized proteins required for synapse development and plasticity. Packaging of these RNAs into DFz2C granules appeared quite specific, as numerous transcripts encoding other synaptic proteins were absent from the foci. The observation that RNAs in DFz2C foci exit the nucleus and that at least one of the transcripts, Par6, is localized to synaptic boutons, suggests that mRNAs exported by nuclear envelope budding translocate to postsynaptic sites for local translation, as has been well documented for large RNA granules in neurons (Wang et al., 2010). However, where such RNA granules are initially formed has not been established. Our results suggest that they could form inside the nucleus.

An important future direction will be to determine whether each granule contains a single mRNA, or is a combination of transcripts. Further, the exact role of DFz2C in assembly and/or transport of granules is at present unclear. Neither is it known whether DFz2C remains associated with the granules after nuclear egress. Intriguingly, DFz2C contains a C-terminal PDZ binding motif, raising the possibility that it may provide a zip code for targeting the granules to postsynaptic sites.

Combined, our results provide novel insight into how synapses communicate with the nucleus to regulate both gene expression and nuclear envelope architecture. In the future it will be of great interest to determine the extent to which the nuclear budding pathway extends to other Wnt receptors and whether it contributes to localized protein expression in response to other signal transduction pathways.

METHODS

A detailed version of the Methods is found in the Supplemental Material

Fly Strains

We used Canton S (CS) (*wild type*), *w;LamC^{EX296} / w;LamC^{EX265}*, *w;;dfz2^{C1} FRT2A / Df(3L)dfz2,w*, UAS-DFz2-RNAi, UAS-LamC-RNAi, UASaPKC-RNAi, UAS-Par6-RNAi, UAS-Baz-RNAi, UAS-DFz2, UAS-PKM, hs-PKM, C57-Gal4, BG487-Gal4, PABP2-GFP, *lamC$^{GFP\text{-}trap/+}$* (G00158). Strain source is specified in the Supplemental Methods.

Immunocytochemistry and Fluorescent Dye Labeling

The following antibodies and markers were used (details on the source and antibody concentration is found in the Supplemental Material): anti-LamC, anti-DFz2-C, mAb414, anti-PABP2, anti-Baz, anti-aPKC, anti-PKC substrate, anti-Horseradish Peroxidase comjugated to Dylight 488, 594, or 649, Alexa Fluor 488 conjugated-Conconavalin-A, Propidium Iodide (PI), Hoechst 3342, texas red-conjugatged 70 KDa dextran, and E36 RNA dye. For PI staining, fixed body wall muscle preparations were first treated with 500 μg/ml RNAse A. TxR-conjugatged dextran was pressure injected into live muscles using a PV380 Pneumatic PicoPump and beveled sharp electrodes.

Image acquisition and analysis

Images were acquired either with a Zeiss LSM5 Pascal confocal or an Improvision spinning disk confocal microscope. Images were deconvolved using measured point spread functions (PSF) and the iterative deconvolution algorithm in the image analysis software package Volocity (Perkin Elmer).

Quantification of foci, ghost boutons, and bouton volume

Nuclear foci were counted at muscles 6 & 7 from abdominal segments A2 and A3 of wandering third instar larvae. The number of foci/nucleus was normalized to simultaneously processed wild type controls. Total number of boutons was quantified in 3rd instar larval preparations double labeled with antibodies to HRP and GluRIII, at segments A3 muscles 6–7. The number of ghost boutons was assessed by counting HRP immunoreactive boutons that were devoid of GluRIII immunoreactivity. Muscle surface was measured by multiplying the width by the length of muscle 6 in segment A3. Bouton volume was quantified using Volocity by cropping the image to individual boutons based on HRP staining, and then using the software to measure volume.

The number of PABP2-GFP and DFz2C foci per nucleus was counted and then plotted against each other. As not all nuclei have a PABP2-GFP or DFz2C foci a Spearman correlation analysis in Prism5 was run on the data (Spearman R=0.52). Analysis of the data with a Generalized Extreme Studentized Deviate (ESD) test suggested there were multiple outliers, which were not excluded. Removing outliers still suggested a significant positive correlation ($p<0.0001$) (Spearman R= 0.44).

Chelerythrine feeding, Lambda phosphatase treatment and heat shock

For Chelerythrine feeding, wild type larvae were raised at low density and transferred to food plates containing either 15μL 26mM Chelerythrine (in water) or 15μL water (control) per 4 ml media and incubated for 21 hours prior to fixing. For lambda phosphatase treatment, larvae were dissected and fixed and then divided between two 0.5mL tubes, one containing 10,000 Units of Lambda protein phosphatase and the other an equal volume of water. After incubation, samples were washed and processed for immunocytochemistry. For

heat shock protocols, mid-late wild type and hs-PKM third instar larvae were collected and either left at room temperature (control) or shifted to 30°C for 30 minutes. Then, they were returned to room temperature for two hours prior to dissection.

Statistical Analysis

Unpaired two-tailed Student's t-tests were run for pairwise comparisons. An unpaired t-test with Welch's correction was performed when variance between samples was significant. For comparison of multiple experimental groups to a control, a one-way ANOVA was performed, with either a Tukey or Dunnet post-hoc tests. Error bars in all graphs represent ±SEM.

E36 RNA dye staining and live imaging

Larval body wall muscles attached to the CNS were dissected in 0.1 mM Ca^{++}-containing HL3 saline, and after incubation in 100 μM E36 (~20 min) and washing, nuclei were imaged by time-lapse microscopy using an Improvision spinning disk confocal microscope. Details on image acquisition and analysis can be found in the Supplemental Material.

Fluorescence In-situ Hybridization (FISH)

The FISH protocol is an adaptation of (Tam et al., 2002). For further details on the protocol and probe preparation, see Supplemental Material.

Electron Microscopy

Transmission electron microscopy was carried out as in (Korkut et al., 2009). Immuno-gold labeling was accomplished by a modification of the protocol by (Yamashita et al., 2009). See Supplemental Material for further details.

Regressive EDTA

Regressive EDTA was conducted as in (Monneron and Bernhard, 1969).

Western Blot

Western blots were carried out as in (Ramachandran et al., 2009).

Supplementary Material

Refer to Web version on PubMed Central for supplementary material.

Acknowledgments

We wish to thank Drs. Thoru Pederson and Jeanne Lawrence for helpful advice and thoughtful discussions. We also thank Dr. Kate Koles and Ms. Yuly Fuentes-Medel for support in some of the molecular studies, as well as Stefanie Kaech Petrie and Aurelie Snyder of the Jungers Center Advance Microscopy Core for help in acquiring and reconstructing the structured illumination images. Finally, we are grateful to the UMassMed Electron Microscopy Facility for support on our ultrastructural studies, and Aaron DiAntonio, Martine Simonelig, and Lori Wallrath for generously sharing antibodies and fly strains. This was work was supported by a Ruth L. Kirschstein NRSA awarded to SDS and NIH grant RO1 NS063228 to VB. Core resources supported by the Diabetes Endocrinology Research Center grant DK32520 were also used. MJM is a HHMI investigator.

LITERATURE CITED

Ataman B, Ashley J, Gorczyca D, Gorczyca M, Mathew D, Wichmann C, Sigrist SJ, Budnik V. Nuclear trafficking of Drosophila Frizzled-2 during synapse development requires the PDZ protein dGRIP. Proc Natl Acad Sci U S A. 2006; 103:7841–7846. [PubMed: 16682643]

Ataman B, Ashley J, Gorczyca M, Ramachandran P, Fouquet W, Sigrist SJ, Budnik V. Rapid activity-dependent modifications in synaptic structure and function require bidirectional wnt signaling. Neuron. 2008; 57:705–718. [PubMed: 18341991]

Benoit B, Nemeth A, Aulner N, Kuhn U, Simonelig M, Wahle E, Bourbon HM. The Drosophila poly(A)-binding protein II is ubiquitous throughout Drosophila development and has the same function in mRNA polyadenylation as its bovine homolog in vitro. Nucleic Acids Res. 1999; 27:3771–3778. [PubMed: 10481015]

Bernhard W. A new staining procedure for electron microscopical cytology. J Ultrastruct Res. 1969; 27:250–265. [PubMed: 4181256]

Betschinger J, Mechtler K, Knoblich JA. The Par complex directs asymmetric cell division by phosphorylating the cytoskeletal protein Lgl. Nature. 2003; 422:326–330. [PubMed: 12629552]

Bjerke SL, Roller RJ. Roles for herpes simplex virus type 1 UL34 and US3 proteins in disrupting the nuclear lamina during herpes simplex virus type 1 egress. Virology. 2006; 347:261–276. [PubMed: 16427676]

Breakefield XO, Kamm C, Hanson PI. Torsin A: movement at many levels. Neuron. 2001; 31:9–12. [PubMed: 11498045]

Budnik V, Salinas PC. Wnt signaling during synaptic development and plasticity. Curr Opin Neurobiol. 2011

Burke B, Stewart CL. Life at the edge: the nuclear envelope and human disease. Nat Rev Mol Cell Biol. 2002; 3:575–585. [PubMed: 12154369]

Buser C, Walther P, Mertens T, Michel D. Cytomegalovirus primary envelopment occurs at large infoldings of the inner nuclear membrane. J Virol. 2007; 81:3042–3048. [PubMed: 17192309]

Cerpa W, Gambrill A, Inestrosa NC, Barria A. Regulation of NMDA-Receptor Synaptic Transmission by Wnt Signaling. J Neurosci. 2011; 31:9466–9471. [PubMed: 21715611]

Darlington RW, Moss LH 3rd. Herpesvirus envelopment. J Virol. 1968; 2:48–55. [PubMed: 4316013]

Davis LI, Blobel G. Identification and characterization of a nuclear pore complex protein. Cell. 1986; 45:699–709. [PubMed: 3518946]

Dickinson HG. Nucleo-Cytoplasmic Interaction following Meiosis in the Young Microspores of Lilium Longiflorum; Events at the Nuclear Envelope. Grana. 1971; 11(2):117–127.

Gay H. Nucleocytoplasmic relations in Drosophila. Cold Spring Harb Symp Quant Biol. 1956; 21:257–269. [PubMed: 13433596]

Gehrig K, Cornell RB, Ridgway ND. Expansion of the nucleoplasmic reticulum requires the coordinated activity of lamins and CTP:phosphocholine cytidylyltransferase alpha. Mol Biol Cell. 2008; 19:237–247. [PubMed: 17959832]

Goodchild RE, Kim CE, Dauer WT. Loss of the dystonia-associated protein torsinA selectively disrupts the neuronal nuclear envelope. Neuron. 2005; 48:923–932. [PubMed: 16364897]

Granata A, Watson R, Collinson LM, Schiavo G, Warner TT. The dystonia-associated protein torsinA modulates synaptic vesicle recycling. J Biol Chem. 2008; 283:7568–7579. [PubMed: 18167355]

Granzow H, Klupp BG, Fuchs W, Veits J, Osterrieder N, Mettenleiter TC. Egress of alphaherpesviruses: comparative ultrastructural study. J Virol. 2001; 75:3675–3684. [PubMed: 11264357]

Haas M, Jost E. Functional analysis of phosphorylation sites in human lamin A controlling lamin disassembly, nuclear transport and assembly. Eur J Cell Biol. 1993; 62:237–247. [PubMed: 7925482]

Hadek R, Swift H. Nuclear extrusion and intracisternal inclusions in the rabbit blastocyst. J Cell Biol. 1962; 13:445–451. [PubMed: 13903455]

Hans S, Freudenreich D, Geffarth M, Kaslin J, Machate A, Brand M. Generation of a non-leaky heat shock-inducible Cre line for conditional Cre/lox strategies in zebrafish. Dev Dyn. 2011; 240:108–115. [PubMed: 21117149]

Herbert JM, Augereau JM, Gleye J, M JP. Chelerythrine is a potent and specific inhibitor of protein kinase C. Biochem Biophys Res Commun. 1990; 172:993–999. [PubMed: 2244923]

Hochstrasser M, Sedat JW. Three-dimensional organization of Drosophila melanogaster interphase nuclei. II. Chromosome spatial organization and gene regulation. J Cell Biol. 1987; 104:1471–1483. [PubMed: 3108265]

Keminer O, Peters R. Permeability of single nuclear pores. Biophys J. 1999; 77:217–228. [PubMed: 10388751]

Kennedy BK, Barbie DA, Classon M, Dyson N, Harlow E. Nuclear organization of DNA replication in primary mammalian cells. Genes Dev. 2000; 14:2855–2868. [PubMed: 11090133]

Klupp BG, Granzow H, Fuchs W, Keil GM, Finke S, Mettenleiter TC. Vesicle formation from the nuclear membrane is induced by coexpression of two conserved herpesvirus proteins. Proc Natl Acad Sci U S A. 2007; 104:7241–7246. [PubMed: 17426144]

Korkut C, Ataman B, Ramachandran P, Ashley J, Barria R, Gherbesi N, Budnik V. Trans-synaptic transmission of vesicular Wnt signals through Evi/Wntless. Cell. 2009; 139:393–404. [PubMed: 19837038]

Kuhn U, Gundel M, Knoth A, Kerwitz Y, Rudel S, Wahle E. Poly(A) tail length is controlled by the nuclear poly(A)-binding protein regulating the interaction between poly(A) polymerase and the cleavage and polyadenylation specificity factor. J Biol Chem. 2009; 284:22803–22814. [PubMed: 19509282]

Lagace TA, Ridgway ND. The rate-limiting enzyme in phosphatidylcholine synthesis regulates proliferation of the nucleoplasmic reticulum. Mol Biol Cell. 2005; 16:1120–1130. [PubMed: 15635091]

Leach NR, Roller RJ. Significance of host cell kinases in herpes simplex virus type 1 egress and lamin-associated protein disassembly from the nuclear lamina. Virology. 2010; 406:127–137. [PubMed: 20674954]

Lee CP, Chen MR. Escape of herpesviruses from the nucleus. Rev Med Virol. 2010; 20:214–230. [PubMed: 20069615]

Li Q, Kim Y, Namm J, Kulkarni A, Rosania GR, Ahn YH, Chang YT. RNA-selective, live cell imaging probes for studying nuclear structure and function. Chem Biol. 2006; 13:615–623. [PubMed: 16793519]

Lim EC, Seet RC. Use of botulinum toxin in the neurology clinic. Nat Rev Neurol. 2010; 6:624–636. [PubMed: 21045798]

Lyu J, Yamamoto V, Lu W. Cleavage of the Wnt receptor Ryk regulates neuronal differentiation during cortical neurogenesis. Dev Cell. 2008; 15:773–780. [PubMed: 19000841]

Maric M, Shao J, Ryan RJ, Wong CS, Gonzalez-Alegre P, Roller RJ. A functional role for torsinA in herpes simplex virus type 1 nuclear egress. J Virol. 2011

Mathew D, Ataman B, Chen J, Zhang Y, Cumberledge S, Budnik V. Wingless signaling at synapses is through cleavage and nuclear import of receptor DFrizzled2. Science. 2005; 310:1344–1347. [PubMed: 16311339]

Mejat A, Decostre V, Li J, Renou L, Kesari A, Hantai D, Stewart CL, Xiao X, Hoffman E, Bonne G, et al. Lamin A/C-mediated neuromuscular junction defects in Emery-Dreifuss muscular dystrophy. J Cell Biol. 2009; 184:31–44. [PubMed: 19124654]

Miech C, Pauer HU, He X, Schwarz TL. Presynaptic local signaling by a canonical wingless pathway regulates development of the Drosophila neuromuscular junction. J Neurosci. 2008; 28:10875–10884. [PubMed: 18945895]

Milbradt J, Webel R, Auerochs S, Sticht H, Marschall M. Novel mode of phosphorylation-triggered reorganization of the nuclear lamina during nuclear egress of human cytomegalovirus. J Biol Chem. 2010; 285:13979–13989. [PubMed: 20202933]

Monneron A, Bernhard W. Fine structural organization of the interphase nucleus in some mammalian cells. J Ultrastruct Res. 1969; 27:266–288. [PubMed: 5813971]

Morin X, Daneman R, Zavortink M, Chia W. A protein trap strategy to detect GFP-tagged proteins expressed from their endogenous loci in Drosophila. Proc Natl Acad Sci U S A. 2001; 98:15050–15055. [PubMed: 11742088]

Mosca TJ, Schwarz TL. The nuclear import of Frizzled2-C by Importins-beta11 and alpha2 promotes postsynaptic development. Nat Neurosci. 2010; 13:935–943. [PubMed: 20601947]

Ostlund C, Bonne G, Schwartz K, Worman HJ. Properties of lamin A mutants found in Emery-Dreifuss muscular dystrophy, cardiomyopathy and Dunnigan-type partial lipodystrophy. J Cell Sci. 2001; 114:4435–4445. [PubMed: 11792809]

Packard M, Koo ES, Gorczyca M, Sharpe J, Cumberledge S, Budnik V. The Drosophila wnt, wingless, provides an essential signal for pre- and postsynaptic differentiation. Cell. 2002; 111:319–330. [PubMed: 12419243]

Park R, Baines JD. Herpes simplex virus type 1 infection induces activation and recruitment of protein kinase C to the nuclear membrane and increased phosphorylation of lamin B. J Virol. 2006; 80:494–504. [PubMed: 16352573]

Petersen SA, Fetter RD, Noordermeer JN, Goodman CS, DiAntonio A. Genetic analysis of glutamate receptors in Drosophila reveals a retrograde signal regulating presynaptic transmitter release. Neuron. 1997; 19:1237–1248. [PubMed: 9427247]

Ramachandran P, Barria R, Ashley J, Budnik V. A critical step for postsynaptic F-actin organization: regulation of Baz/Par-3 localization by aPKC and PTEN. Dev Neurobiol. 2009; 69:583–602. [PubMed: 19472188]

Reynolds AE, Liang L, Baines JD. Conformational changes in the nuclear lamina induced by herpes simplex virus type 1 require genes U(L)31 and U(L)34. J Virol. 2004; 78:5564–5575. [PubMed: 15140953]

Robottom BJ, Weiner WJ, Comella CL. Early-onset primary dystonia. Handb Clin Neurol. 2011; 100:465–479. [PubMed: 21496603]

Roller RJ. Nuclear egress of herpes viruses. Virologica Sinica. 2008; 23:406–415.

Ruiz-Canada C, Ashley J, Moeckel-Cole S, Drier E, Yin J, Budnik V. New Synaptic Bouton Formation Is Disrupted by Misregulation of Microtubule Stability in aPKC Mutants. Neuron. 2004; 42:567–580. [PubMed: 15157419]

Ryckman BJ, Roller RJ. Herpes simplex virus type 1 primary envelopment: UL34 protein modification and the US3-UL34 catalytic relationship. J Virol. 2004; 78:399–412. [PubMed: 14671121]

Schulze SR, Curio-Penny B, Li Y, Imani RA, Rydberg L, Geyer PK, Wallrath LL. Molecular genetic analysis of the nested Drosophila melanogaster lamin C gene. Genetics. 2005; 171:185–196. [PubMed: 15965247]

Schulze SR, Curio-Penny B, Speese S, Dialynas G, Cryderman DE, McDonough CW, Nalbant D, Petersen M, Budnik V, Geyer PK, et al. A comparative study of Drosophila and human A-type lamins. PLoS ONE. 2009; 4:e7564. [PubMed: 19855837]

Siegfried E, Perrimon N. Drosophila wingless: a paradigm for the function and mechanism of Wnt signaling. Bioessays. 1994; 16:395–404. [PubMed: 8080429]

Sigrist SJ, Thiel PR, Reiff DF, Lachance PE, Lasko P, Schuster CM. Postsynaptic translation affects the efficacy and morphology of neuromuscular junctions. Nature. 2000; 405:1062–1065. [PubMed: 10890448]

Speese SD, Budnik V. Wnts: up-and-coming at the synapse. Trends Neurosci. 2007; 30:268–275. [PubMed: 17467065]

Szollosi D. Extrusion of nucleoli from pronuclei of the rat. J Cell Biol. 1965; 25:545–562. [PubMed: 5320297]

Szollosi MS, Szollosi D. 'Blebbing' of the nuclear envelope of mouse zygotes, early embryos and hybrid cells. J Cell Sci. 1988; 91((Pt 2)):257–267. [PubMed: 3267698]

Tam, R.; Shopland, LS.; Johnson, CV.; McNeil, J.; Lawrence, JB. Applications of RNA FISH for visualizing gene expression and nuclear architecture. In: Beatty, BMSSJ., editor. FISH Practical Approach. New York: Oxford University Press; 2002. p. 93-118.

Varela-Nallar L, Alfaro IE, Serrano FG, Parodi J, Inestrosa NC. Wingless-type family member 5A (Wnt-5a) stimulates synaptic differentiation and function of glutamatergic synapses. Proc Natl Acad Sci U S A. 2010; 107:21164–21169. [PubMed: 21084636]

Wang DO, Martin KC, Zukin RS. Spatially restricting gene expression by local translation at synapses. Trends Neurosci. 2010; 33:173–182. [PubMed: 20303187]

Wu CF, Ganetzky B, Haugland FN, Liu AX. Potassium currents in Drosophila: different components affected by mutations of two genes. Science. 1983; 220:1076–1078. [PubMed: 6302847]

Yamashita S, Katsumata O, Okada Y. Establishment of a standardized post-embedding method for immunoelectron microscopy by applying heat-induced antigen retrieval. J Electron Microsc (Tokyo). 2009; 58:267–279. [PubMed: 19332863]

Zhang H, Zha X, Tan Y, Hornbeck PV, Mastrangelo AJ, Alessi DR, Polakiewicz RD, Comb MJ. Phosphoprotein analysis using antibodies broadly reactive against phosphorylated motifs. J Biol Chem. 2002; 277:39379–39387. [PubMed: 12151408]

Article highlights

- Synaptic Wnt controls postsynaptic gene expression through novel nuclear export.
- Wnt receptor fragments organize ribonucleoprotein (RNP) particles in the nucleus.
- RNP particles consist of specific transcripts required for new synapse formation.
- RNP particles bud through nuclear envelope similar to Herpes virus nuclear export.

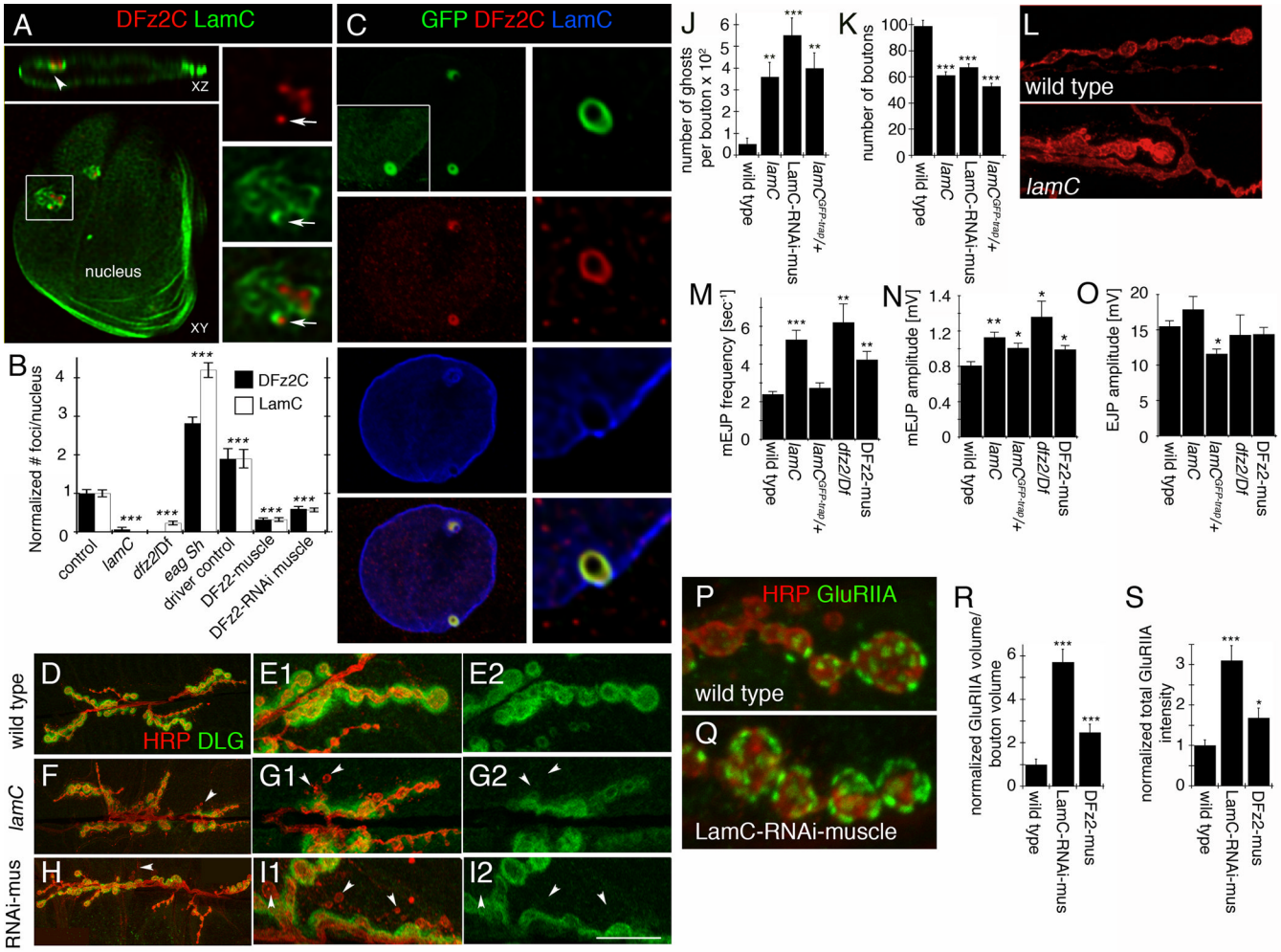

Figure 1. Subnuclear localization of DFz2C and LamC at larval muscle nuclei and defective NMJs in *lamC* mutants (also see SF1)

A- LamC and DFz2C labeling (deconvolved) of muscle nucleus containing a DFz2C/LamC focus (box; enlarged in right panels) localized to the nuclear periphery (arrowhead in XZ plane). Arrows=DFz2C granule within the LamC framework-like structure.

B- Number of DFz2C and LamC foci/nucleus. N (same order as in graph)=450, 413, 302, 530, 328, 617, 593.

C- Localization of LamC-GFP and wild type LamC in muscle nucleus from *lamC*$^{GFP\text{-}trap/+}$ in relationship to DFz2C (box; enlarged in right panels). Inset is the same nucleus but overexposed.

Calibration=5μm A (left), 2μm A and C (right), 7μm C (left). Images are single confocal slices.

D–I- Larval NMJsdouble labeled with antibodies to HRP and DLG in

D,E- a wild type NMJ at (**A**) low and (**B**) high magnification,

F, G- a *lamC* null mutant NMJ at (**C**) low and (**D**) high magnification, and

H, I- an NMJ from a larva expressing LamC-RNAi in muscles (LamC-RNAi-muscle).

Arrowheads=ghost boutons. Calibration=30μm **D, F, H**; 12μm **E, G, I**.

J, K- Morphometric analysis of NMJs showing

J- ghost boutons, and

K- bouton number.

N (same order as in graph)= 10, 19, 16, 16.
L- Morphology of synaptic boutons in (**top**) wild type and (**bottom**) *lamC* mutant. Calibration=12μm.
M–O- Electrophysiological analysis of larval NMJs showing

M- mEJP frequency,

N- mEJPs amplitude, and

O- evoked EJP amplitude.

N (same order as in graph)=8, 8, 5, 5, 7.
P,Q- Larval NMJs labeled with HRP and DGluRIIA antibodies in

(**P**) wild type and

(**Q**) a larva expressing LamC-RNAi in muscles.

Calibration= 5 μm.
R,S- Morphometric analysis of GluRIIA clusters showing

(**R**) GluRIIA label volume and

(**S**) total intensity.

***= $p< 0.0001$; **= $p<0.01$; *= $p<0.05$. Bars in graphs indicate mean±SEM.

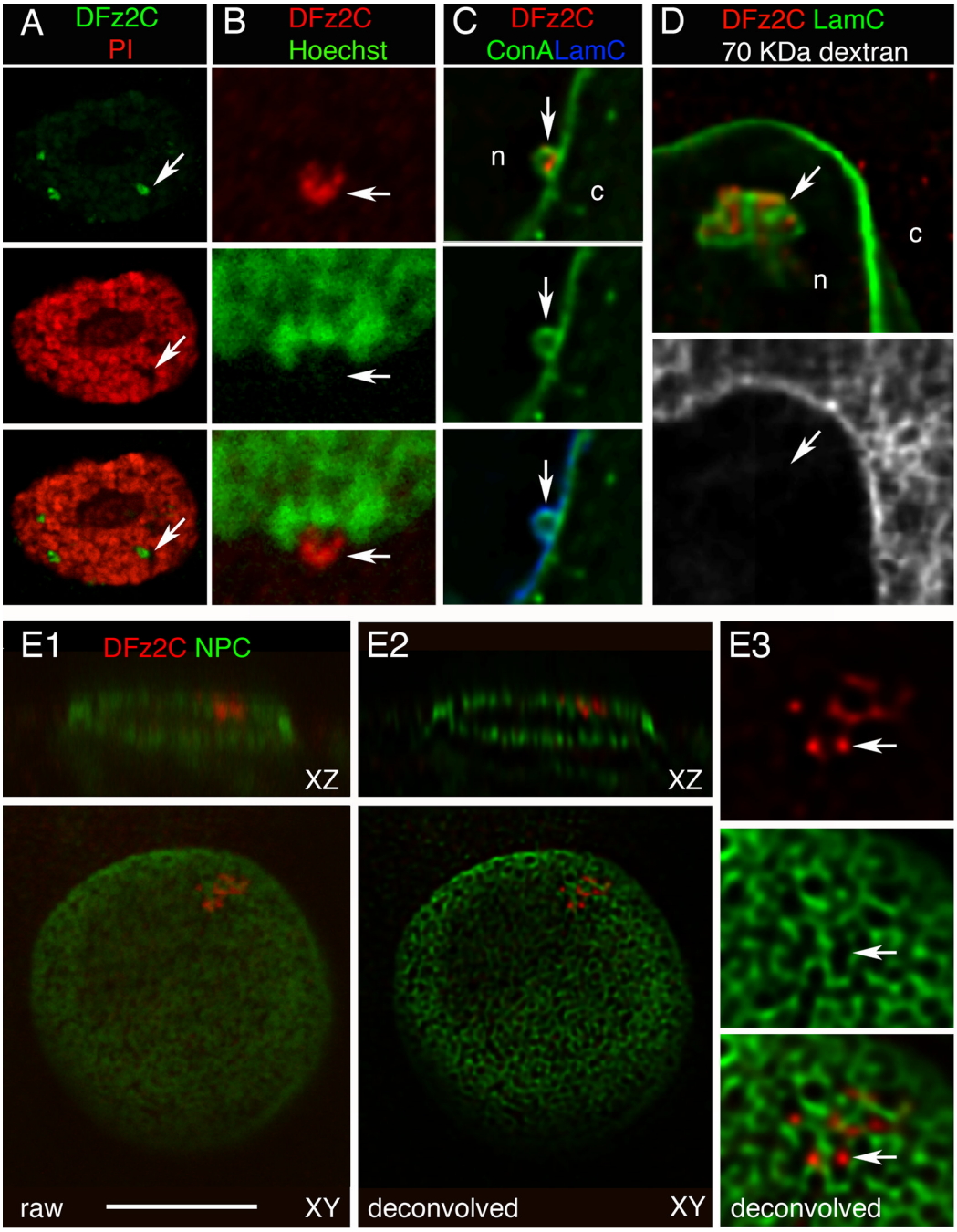

Figure 2. Localization of DFz2C/LamC foci at larval muscle nuclei in relationship to DNA, nuclear membrane, nuclear pore complexes, and cytoplasmic 70 KDa-dextran (also see SF1,2)

A–E- DFz2C/LamC foci (arrows) in relationship with

A, B- propidium iodide and Hoechst,

C- the membrane marker Concanavalin-A (ConA; deconvolved),

D- 70 KDa dextran injected into the cytoplasm (deconvolved),

E- mAb414 labeling the nuclear pore complex (NPC;(Davis and Blobel, 1986)).

E1 shows a raw image of the nucleus,

E2 a deconvolution of **E1**, and

E3 a high magnification view of the focus in **E2**.

Images are single confocal slices; c= cytoplasm; n=nucleoplasm; Calibration= 14μm **A**; 8μm **B, E1–2**; 4μm **C, D, E3**.

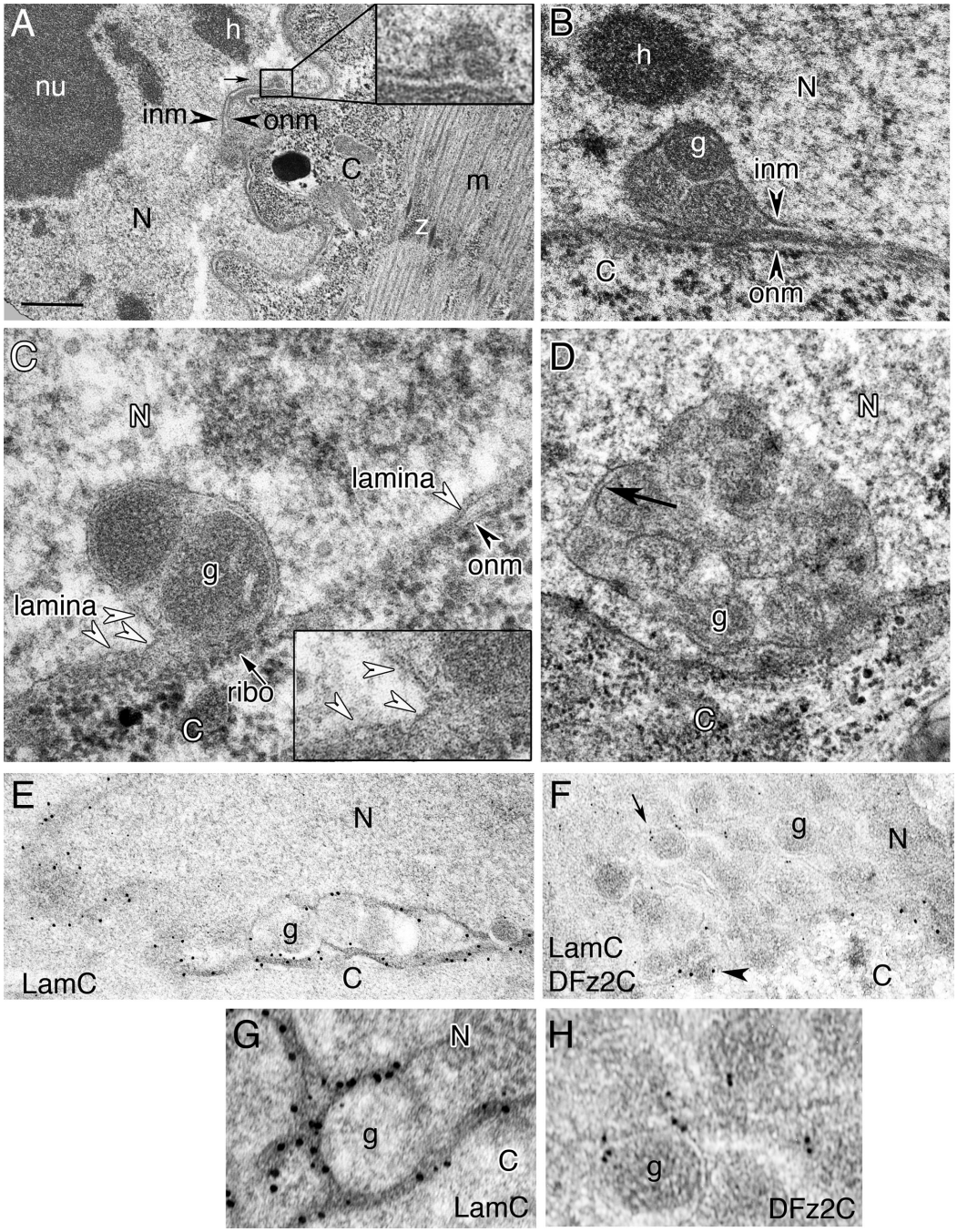

Figure 3. Ultrastructural organization of DFz2C/LamC foci (also see SF3

Transmission electron micrographs of larval muscle or S2 cell nuclei containing DFz2C/LamC foci.

A- Low magnification of a focus (box; enlarged in inset) within a muscle nucleus.

B–D- High magnification of INM invaginations containing electron dense granules (g) from

B- larval muscle.

C, D- S2 cells. Dense granules appear to be bounded by membrane (arrow in **D**).

E–H- Immunoelectron micrographs of muscle nuclei labeled with

E, G- anti-LamC and 18nm gold-conjugated second antibody shown at (**E**) low and (**G**) high magnification;

F, H- anti-DFz2C and anti-LamC with 12nm and 18nm gold conjugated second antibody, respectively, shown at (**F**) low and (**G**) high magnification.

N= nucleus; C= cytoplasm; nu= nucleolus; h=heterochromatin; inm= inner nuclear membrane; onm= outer nuclear membrane; m= myofibrils; z= perforated z band. Calibration=0.5μm **A**; 0.3μm **B, D**; 0.4μm **E, F**; 0.1μm **C, G, H**.

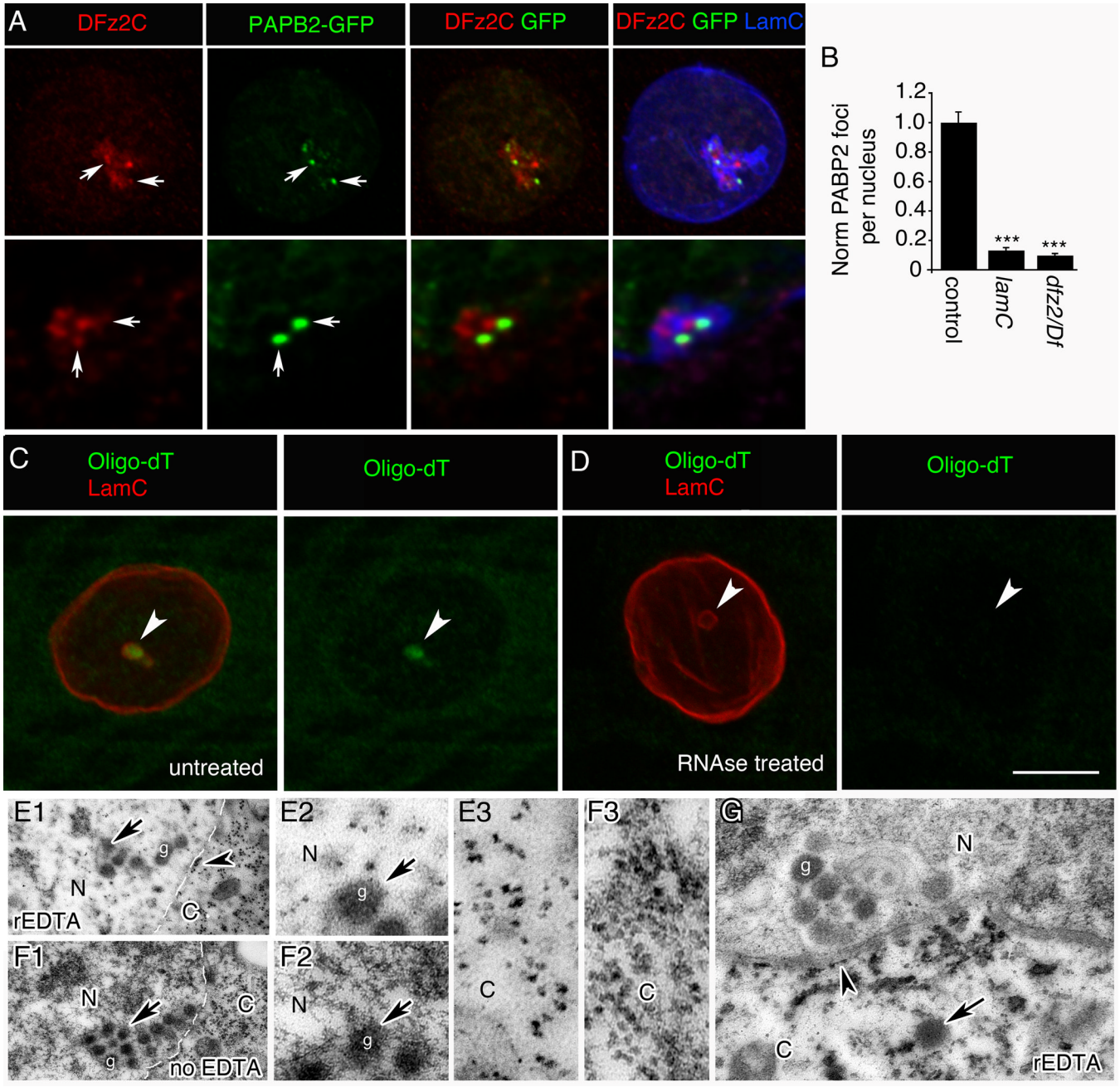

Figure 4. PABP2 and poly(A) RNA are associated with DFz2C/LamC foci (also see SF4)

A- View of a muscle nucleus showing the relationship between DFz2C/LamC and PABP2-GFP foci (arrows), displayed at (**top**) low and (**bottom**) high (deconvolved) magnification.

B- PABP2 foci number/muscle nuclei. N (same order as in graph)=229, 175, 301.

C, D- Muscle nucleus labeled with poly(dT) FISH and anti-LamC, either

C- without or

D- with RNase treatment.

E–G- View of muscle DFz2/LamC foci in sections

E- treated with rEDTA and

F- not treated with EDTA (same preparation as in (**E**)). N= nucleus; C= cytoplasm.

E2, F2- High magnification views at the nuclear area of E1 and F1 around a DFz2C granule showing a dark meshwork surrounding the granule, which is bleached after rEDTA treatment (E2), while DFz2C granules retain electron density (F2).

E3, F3- High magnification of E1 and F1, showing ribosomes in the cytoplasm, which retain electron density after EDTA treatment.

G- Low magnification view of a muscle focus showing retention of electron density by DFz2C granules after rEDTA (g; arrow).

Arrowheads=ribosomes at ONM. Arrow=cytoplasmic granule of the same size and morphology as DFz2C granules at INM invaginations.

Calibration= 8μm **A** (top row); 3μm **A** (bottom row); 8μm **C**, **D**; 0.6μm **E1, F1**; 0.2μm **E2–3, F2–3**; 1μm **G**.
***= $p < 0.0001$. Bars in graphs indicate mean±SEM.

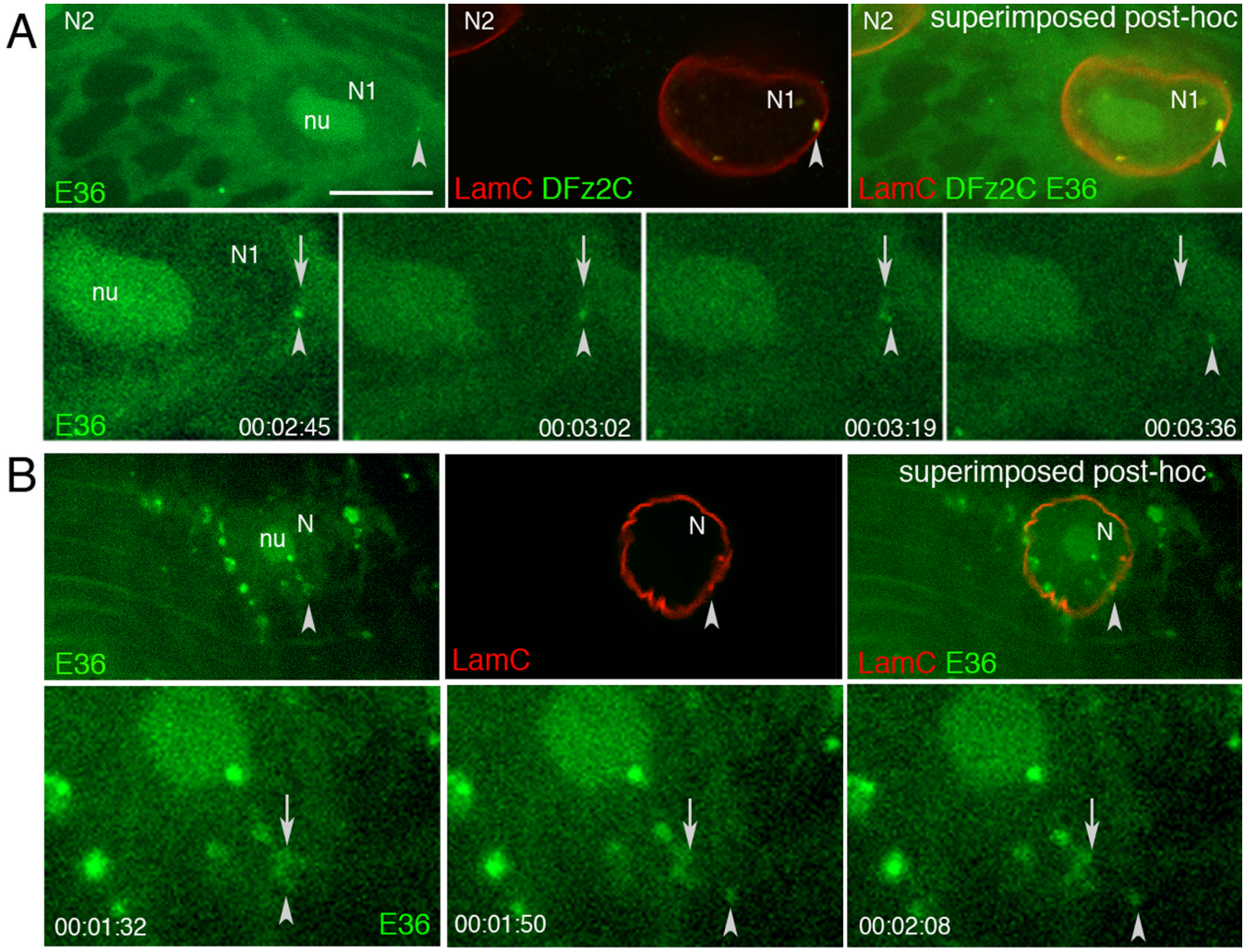

Figure 5. RNA granules from DFz2C/LamC foci exit larval muscle nuclei

A, B- Nuclei imaged live from larval body wall muscle preparations after incubation with E36 RNA dye. After time-lapse imaging, samples were fixed and labeled with antibodies to DFz2C and/or LamC. N=nucleus; nu=nucleolus. See Supplementary Movie 1 and 2. Calibration=10μm **A**(top row), **B**(top row); 4μm **A**(bottom row), **B**(bottom row).

Top rows in **A, B** show (top panel) a single image of a larval body wall muscle nucleus labeled with E36, (middle panel) the same nucleus after fixation and immunolabeling with DFz2C and/or LamC antibodies, and (right panel) their superposition obtained after resizing using fiduciary markers. Arrowheads=position of the E36 and DFz2C/LamC foci.

Bottom rows in **A, B** display time-lapse imaging series, showing an E36 labeled granule exiting the nucleus of a larval body wall muscle. Arrows = initial position of the granule; arrowheads= granules while moving away from the nucleus. Time marks=hr:min:sec.

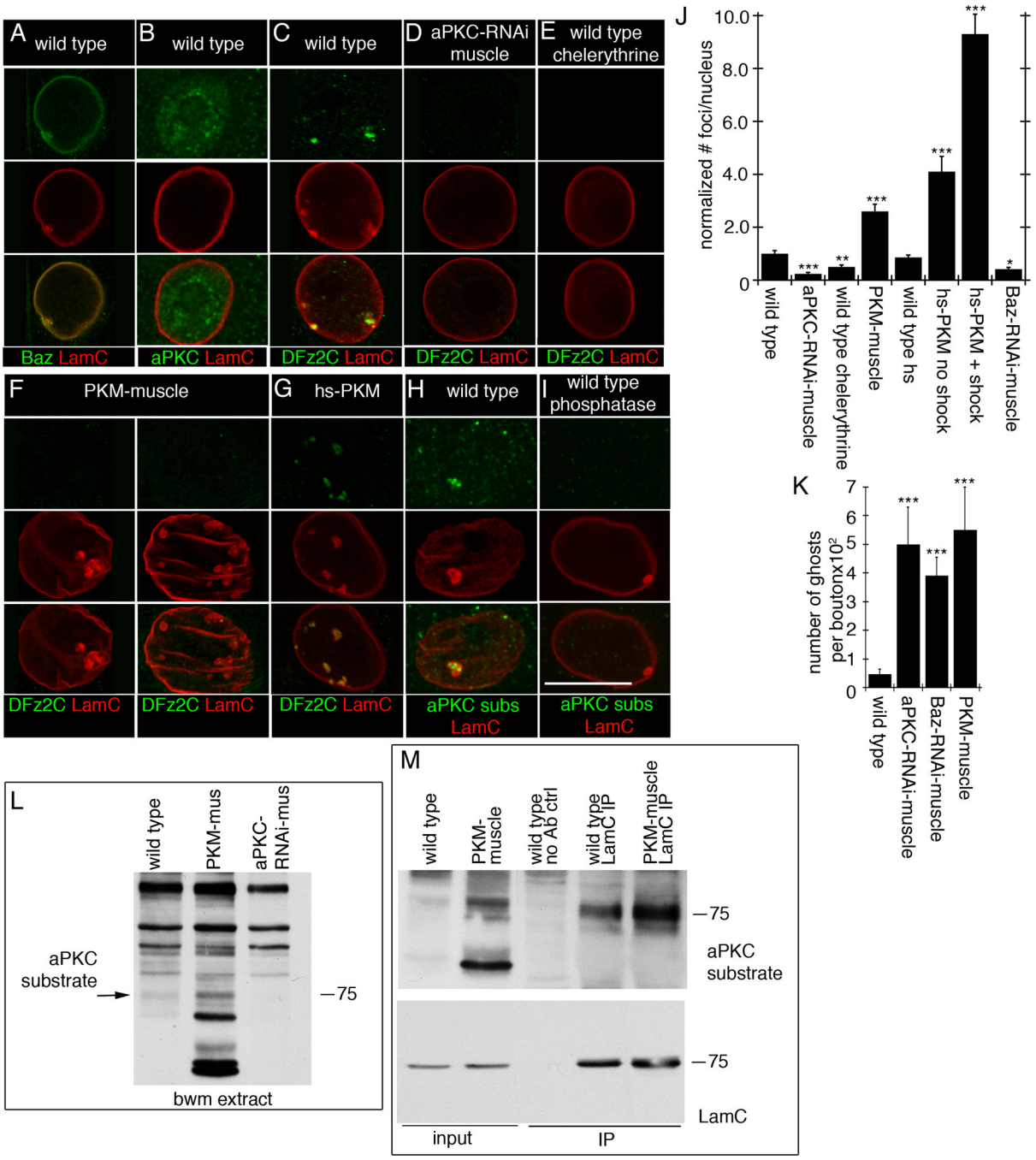

Figure 6. aPKC is required for foci formation (also see SF5)

A–I- Body wall muscle nuclei labeled with antibodies to either Baz, aPKC, PKC-phosphorylated substrate (aPKC subs), or DFz2C, double labeled with antibodies to LamC in wild type and genetic variants altering aPKC activity showing

A- localization of Baz at LamC foci,

B- diffuse distribution of aPKC in muscle nuclei,

C- a DFz2C/LamC foci in wild type muscle nucleus,

D- virtual elimination of DFz2C/LamC foci by expressing aPKC-RNAi in muscles,

E- that chelerythrine feeding, decreases DFz2C/LamC foci,

F- that expressing PKM in muscles enlarges and increases LamC foci number, which are devoid of DFz2C,

G- that expressing PKM for just 30 min increases DFz2C/lamC foci number,

H- enrichment of PKC phosphorylated substrates immunoreactivity at LamC foci, and

I- that this label is eliminated after treatment with lambda phosphatase.

Calibration=15μm.
J- Foci number per nuclei upon altering aPKC activity. N (same order as in graph)=2146, 532, 726, 677, 713, 601, 595, and 652.
K- Ghost bouton number in indicated genotypes. N=6 for each genotype.
L- Western blot of body wall muscle extracts probed with anti-P-PKCs, showing a band of the same molecular weight as LamC (arrow) which increases in intensity in PKM-muscle extracts, and which decreases in intensity in aPKC-RNAi-muscle extracts. N=3.
M- Immunoprecipitation of body wall muscle extracts with LamC antibody. N=3.
***= $p < 0.0001$; **= $p < 0.01$; *= $p < 0.05$. Bars in graphs indicate mean±SEM.

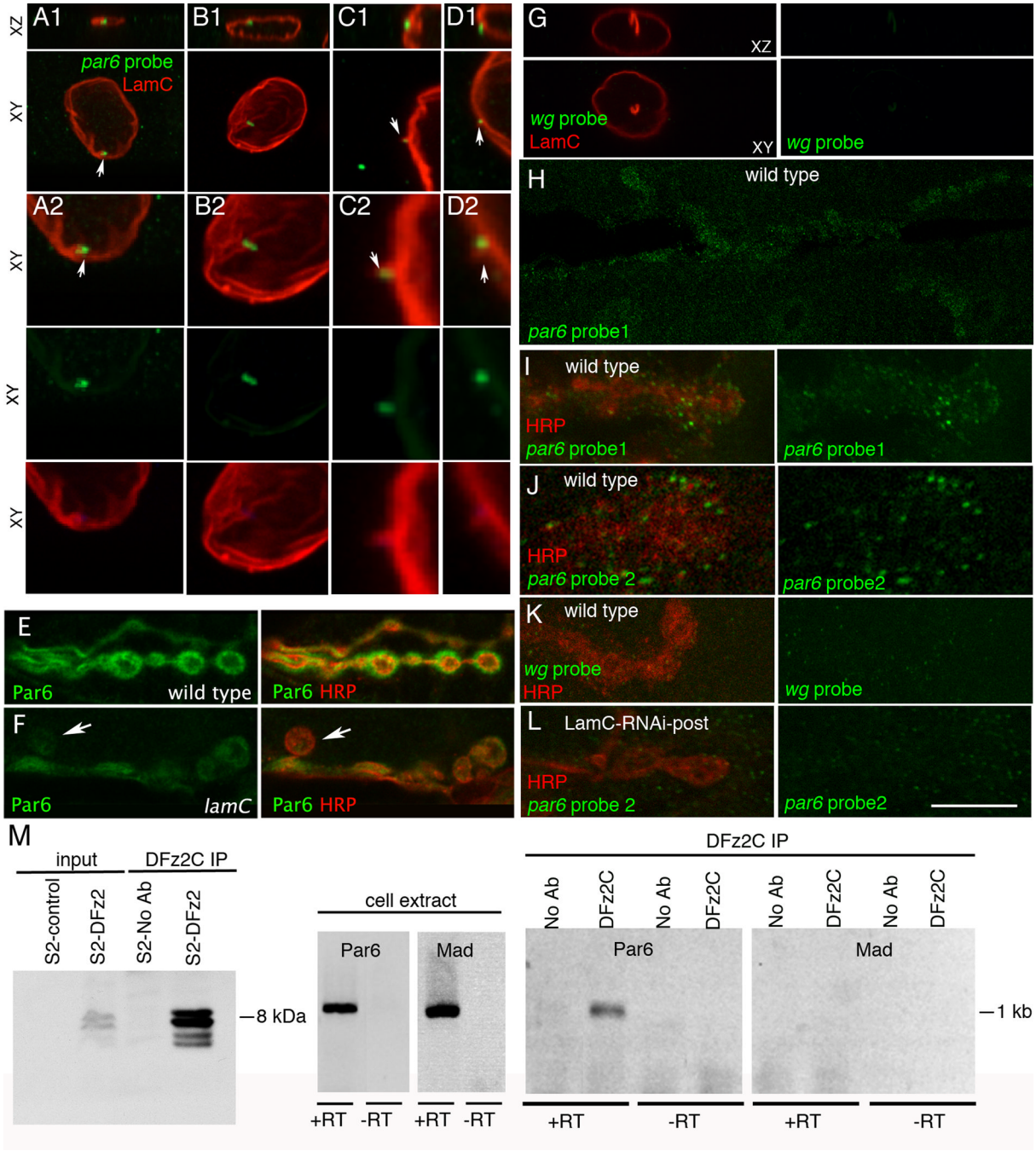

Figure 7. *par6* transcript is localized to LamC foci and the NMJ, and forms a complex with DFz2C (also see SF5,6)

A–D, G-L *In situ* hybridization to larval body wall muscles using *par6* or *wg* probes showing

A- association of *par6* mRNA with a LamC focus (arrow);

B- localization of *par6* transcript near a nuclear membrane fold;

C, D- localization of *par6* transcript to cytoplasmically directed projections of the nuclear boundary.

A2–D2 are high magnification views of the nuclei shown in **A1–D1**.

G- Absence of FISH signal when using a *wg* probe;

H- a low magnification view of *par6* mRNA at the postsynaptic larval NMJ;

I–J synaptic *par6* mRNA localization using 2 different *par6* probes;

K- absence of synaptic *wg* mRNA localization;

L- synaptic *par6* mRNA localization in a larva expressing LamC-RNAi in muscle, showing virtual elimination of postsynaptic *par6* mRNA.

E–F- Larval NMJs labeled with antibodies against HRP and Par6 in

E- wild type and

F- *lamC* mutant showing a ghost bouton (arrow) devoid of Par6 immunoreactivity and a general decrease in Par6 levels throughout the NMJ.

Calibration =15μm **A1, B1, G**; 7μm **A2, B2**; 5μm **C1, D1, J**; 2.5μm **C2, D2**; 20μm **H**; 10μm **E, F, I, K, L**.
M- Immunoprecipitation of *par6* RNA using anti-DFz2C. Left: immunoprecipitation of DFz2C fragment using anti-DFz2C. Middle: RT-PCR from S2 cell RNA. Right: RT-PCR of the DFz2C immunoprecipitate.